

Dynamic Globularization Behavior of O-phase Lamellae in Ti-22Al-25Nb (at%) Alloy during Deformation at Elevated Temperatures

Lin Peng^{1,2}, Tang Tingting¹, Chi Chengzhong^{1,2}, Zhang Shuzhi^{1,2}, Zhang Changjiang^{1,2}

¹ College of Materials Science and Engineering, Taiyuan University of Technology, Taiyuan 030024, China; ² Shanxi Key Laboratory of Advanced Magnesium-based Materials, Taiyuan University of Technology, Taiyuan 030024, China

Abstract: To clarify the globularization mechanism and model of the O-phase lamellae of Ti₂AlNb-based alloys during deformation at elevated temperatures, the hot deformation behavior and microstructure evolution of Ti-22Al-25Nb (at%) alloy during hot compression deformation in (α_2 +O+B2) region were investigated. The results show that the flow softening is relevant to the dynamic globularization of O-phase lamellae and the flow instability including 45° shear deformation, 45° shear cracking and micro-cracks. The deformation constitutive model based on the exponential law was established and the deformation activation energy was calculated to be 831 kJ·mol⁻¹. The globularization of O-phase lamellae is hard to occur at low temperatures or at high strain rates due to slow diffusion rate or insufficient diffusion time. The main globularization mechanism is the kink and shear of the O-phase lamellae, which is confirmed to be a dynamic recrystallization behavior. The dynamic globularization kinetics was also studied, which is sensitive to deformation conditions including deformation temperatures and strain rates and follows an Avrami type sigmoid equation.

Key words: Ti₂AlNb alloy; dynamic globularization; dynamic recrystallization; hot deformation

In recent years, Ti₂AlNb-based alloys have been extensively used in aerospace field due to their attractive properties such as low density, high strength-to-density, good oxidation resistance and nonmagnetic property^[1-4]. A Ti₂AlNb-based alloy with the composition of Ti-22Al-25Nb (at%) is an important member of this alloy group, which has been proved to have good mechanical properties at room and elevated temperatures^[2,5].

Due to limited formability of the alloy at room temperature, it is advisable to form them into desired shapes at elevated temperatures. For some aerospace components with complex geometries and intricate designs, the forming temperature is often set over 930 °C^[6], which is in (α_2 +O+B2) phase region in Ti-Al-Nb ternary phase diagram^[7,8]. When deforming in this phase region, Ti₂AlNb-

based alloys may exhibit strong microstructure instability induced by dynamic phase transformation, coarsening and globularization of O-phase lamellae, etc., which may lead to substantial changes in the initial mechanical properties, such as the yield strength and creep resistance^[8]. Hence, the phenomenological and mechanistic descriptions of such microstructural changes is of significance whether from scientific or engineering perspectives^[9]. For Ti₂AlNb-based alloys, the static instability of the O-phase during the elevated-temperature exposure has been examined both experimentally and theoretically^[1,7,10]. Lin et al.^[8] qualitatively characterized the coarsening, fragmentation, and globularization of the O-phase lamellae during elevated-temperature deformation. However, the globularization model of the O-phase lamellae has not been quantitatively

Received date: February 14, 2017

Foundation item: National Natural Science Foundation of China (51505323, 51504163)

Corresponding author: Lin Peng, Ph. D., Lecturer, College of Materials Science and Engineering, Taiyuan University of Technology, Taiyuan 030024, P. R. China, , E-mail: linpeng@tyut.edu.cn

Copyright © 2018, Northwest Institute for Nonferrous Metal Research. Published by Elsevier BV. All rights reserved.

studied until now.

The purpose of the present study is to investigate the hot deformation behavior and microstructure evolution of Ti-22Al-25Nb (at%) alloy during hot compression deformation, aiming at clarifying the globularization mechanism and model of the O-phase lamellae during deformation in (α_2 +O+B2) phase region. It is expected that the results can provide a good guideline for microstructure control during hot forming of this alloy group.

1 Experiment

The experimental Ti-22Al-25Nb (at%) alloy was provided by Central Iron and Steel Research Institute (CISRI) in the form of a bar with a diameter of 85 mm. The chemical analysis showed that the composition of the alloy is in good agreement with the nominal composition (Table 1). The microstructure of the as-received bar is shown in Fig.1, which exhibits a typical basket-weave microstructure.

Cylindrical specimens with 8 mm in height and 12 mm in diameter were machined along the compression axis on the low-speed wire electrical discharge machine. In order that the friction could be reduced during the compression tests, concentric grooves of 0.2 mm in depth were machined at both ends of the specimens to effectively facilitate the retention of the glass lubricant. The hot compression tests were carried out on a Gleebe-3500 thermo-mechanical simulator at temperatures of 930, 950 and 970 °C, and strain rates of 0.001, 0.01, 0.1 and 1 s⁻¹. The height reduction was set as 10%, 30%, 50% and 70%. Deformed specimens were axially sectioned parallel to the compression axis and the cut surface was prepared for metallographic examination using

conventional techniques. The microstructure of compressed specimens was directly observed by scanning electron microscope (SEM) and transmission electron microscope (TEM). The globularization behavior of O-phase lamellae was then quantified using moderate magnification SEM by a quantitative metallographic image analysis system (Image-pro plus 5.0) considering O-phase morphology with the Feret ratio (Feretmax/Feretmin) lower than 2.5 as globular.

2 Results and Discussion

2.1 Flow behavior

The stress-strain curves of the alloy deformed at various temperatures and strain rates are shown in Fig.2.

Table 1 Chemical composition of Ti-22Al-25Nb alloy (at%)

Ti	Al	Nb	O	N	H
Bal.	22.3	25.7	4.30×10^{-4}	5.2×10^{-5}	9×10^{-6}

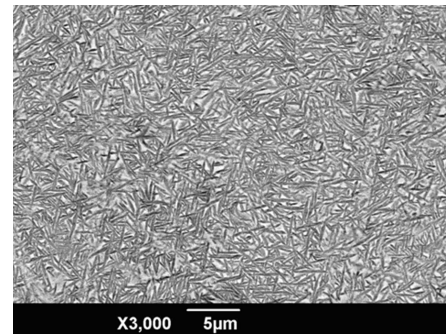


Fig.1 Microstructure of the as-received Ti-22Al-25Nb alloy

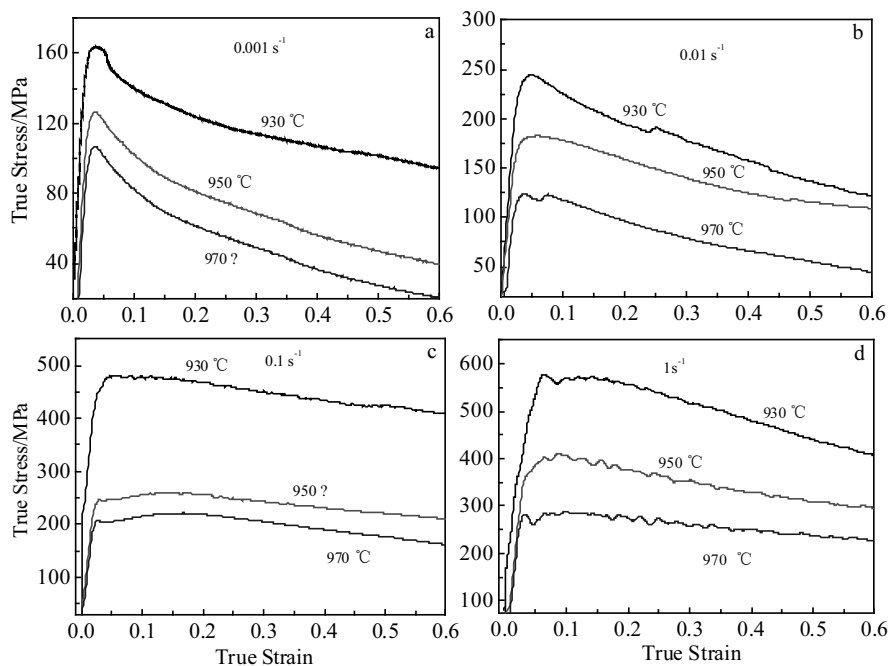


Fig.2 Stress-strain curves of alloy deformed at various temperatures and strain rates of 0.001 s⁻¹ (a), 0.01 s⁻¹ (b), 0.1 s⁻¹ (c), and 1 s⁻¹ (d)

First, the flow stress increases sharply to a peak with strain increasing at the beginning of deformation, and then decreases with the strain further increasing. This behavior is termed as discontinuous yielding^[11,12], a common phenomenon for many titanium alloys. The strain for the peak stress is in the range of 0.01~0.04 and increases with increase in the strain rate or decrease in the deformation temperature. The variation of the peak stress and the corresponding strain confirms the strong sensitivity of the flow stress to strain rate and deformation temperature, which is associated with the microstructure changes during deformation.

Discontinuous yielding is attributed to the generation of new mobile dislocations from grain boundary sources, and this effect depends on both type and concentration of β phase stabilizing elements^[12-14]. The discontinuous yielding phenomenon of the alloy was observed obviously as the strain rate increased, in accordance with the results for Ti-10V-2Fe-3Al (wt%) alloy and Ti-4Al-4Mo-2Sn-0.5Si (wt%) alloy by Robertson and Meshan^[15]. This behavior often results from competition between the work-hardening and dynamic softening. The propagation and piling of dislocations result in the work-hardening effect, which is much stronger than the dynamic softening effect at the beginning of deformation. After the flow stress reaches a peak value, the dynamic softening effect becomes superior to the work hardening effect, leading to the decrease of flow stress with the strain increasing.

In addition, flow softening occurs after the flow stress reaches the peak value and exhibits significant oscillatory flow at higher strain rates and lower temperatures. The adiabatic shear band at an angle of 45° to the compression axis emerges when the alloy is compressed at strain rate of 1 s⁻¹ and height reduction of 50% (Fig.3a). The micro-cracks are also seen in Fig.3b when the alloy is compressed at 930 °C and strain rate of 1 s⁻¹. Therefore, those broad oscillations should be induced by this instable deformation^[16]. The flow softening rate is also more apparent during low temperature and high strain rate deformation. It is because Ti₂AlNb-based alloys have low thermal conductivity, leading to inadequate heat dissipation during hot working and thus a significant local temperature rise appears, especially at low temperatures or high strain rates. Therefore, the local temperature rise plays a dominant role in the flow softening. Moreover, the dynamic recrystallization or recovery, voids and cracks formation, etc. can also result in flow softening. Therefore, the deformation mechanism of the alloy can not be accurately determined in terms of only the shapes of the stress-strain curves because different microstructural mechanisms of hot deformation may result in similar stress-strain behaviors. Furthermore, the flow stress of Ti-22Al-25Nb (at%) alloy decreases very quickly when the strain rate is low, as shown

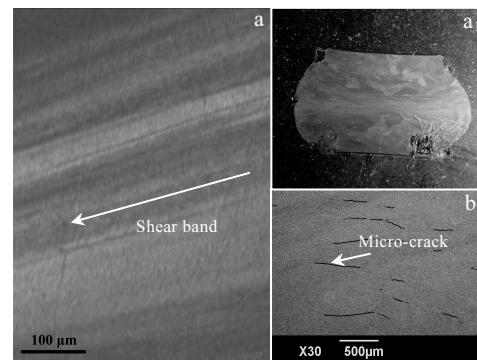


Fig.3 Shear bands at an angle of 45° to the compression axis (a, a₁) and micro-cracks (b)

in Fig.2a and 2b, and the decreasing rate increases with the deformation temperature increasing. This phenomenon is different from the traditional titanium alloys, such as Ti60^[17] and TC21^[18] alloys, of which the stress keeps nearly a constant when the alloys are compressed at low strain rates (0.001 and 0.01 s⁻¹). This may be related to the dynamic globularization of the O-phase lamellae during deformation. The details about the dynamic globularization of the O-phase lamellae will be discussed subsequently.

2.2 Constitutive model of deformation

The dependence of the flow stress on strain rate and temperature can be expressed in the forms of an Arrhenius kinetic rate equation^[19]:

$$\dot{\epsilon} = A \sigma^n \exp(-Q/RT) \quad (1)$$

Where A is the material constant, $\dot{\epsilon}$ is the strain rate (s⁻¹), Q is the apparent activation energy for deformation (kJ·mol⁻¹), σ is the flow stress (MPa), T is the absolute deformation temperature (K), R is the gas constant (8.3145 J/mol·K) and n is the stress exponent.

Relationship between the peak flow stress and strain rate in (α_2 +O+B2) region during hot deformation are shown in Fig.4a. The stress exponent n is calculated from the inverse of the slope of the $\ln \sigma - \ln \dot{\epsilon}$ plot. n is equal to 5.7 by linear regression based on the Origin8.0 software. Fig.4b shows the peak flow stress in dependence of the deformation temperature at different strain rates. The estimated value of the average activation energy (Q) for Ti-22Al-25Nb alloy in (α_2 +O+B2) region is calculated as 831 kJ·mol⁻¹. Q of Ti₂AlNb-based alloys has been examined for the creep deformation, ranging from 250~450 kJ·mol⁻¹ [20-22], smaller than that of this study. Seshacharyulu^[23] indicated that the high activation energy is related to the breakup or globularization of lamellar phases.

Fig.5 shows that both factors exist for the current alloy. The higher activation energy means the more difficult activation of the deformation for the alloy. The constitutive equation can be described as:

$$\dot{\epsilon} = 7 \times 10^{21} \sigma^{5.7} \exp(-831/RT) \quad (2)$$

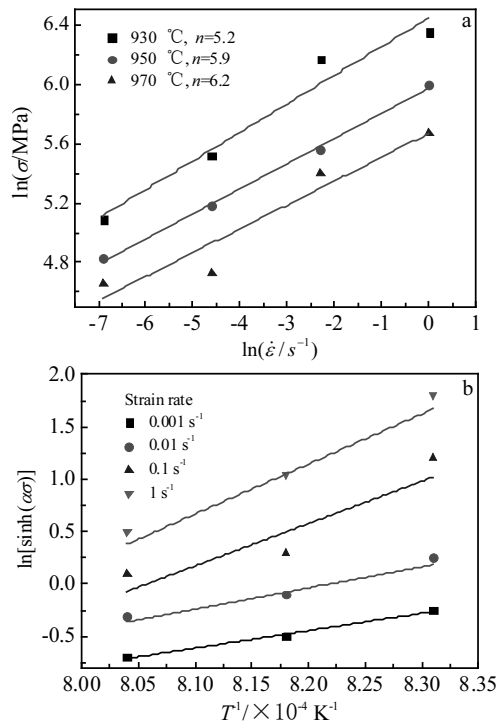


Fig.4 Relationship of the peak flow stress to strain rates (a) and to temperatures (b)

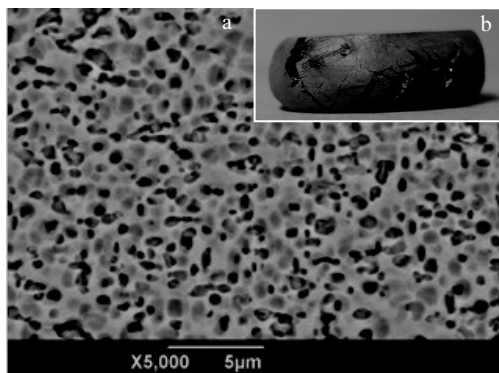


Fig.5 Globularization of the O-phase lamellae and shear breakup at an angle 45° to the compression axis (inset)

The effect of deformation temperature and strain rate on the peak flow stress can be expressed by the Zener-Hollomon parameter abbreviated as Z as follows:

$$Z = \dot{\epsilon} \exp(Q/RT) \quad (3)$$

Variation of the peak flow stress with Zener-Hollomon parameter for the current alloy is shown in Fig.6. The correlation coefficient r for the linear regression of $\ln Z - \ln \sigma$ plot is 0.94, indicating a good linear correlation between the flow stress and Z value.

2.3 Dynamic globularization model

Fig. 7a~7c show the microstructures of samples compressed at different temperatures with a low strain rate of 0.001 s⁻¹ and height reduction of 30%.

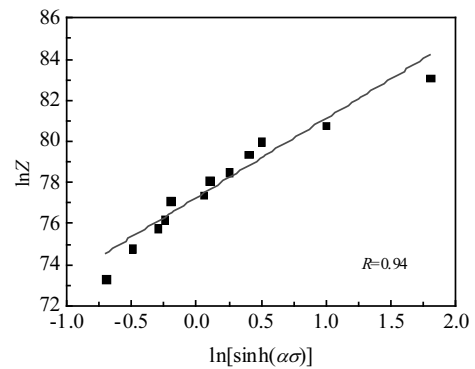


Fig.6 Relationship between peak flow stress and Zener-Hollomon parameter for Ti-22Al-25Nb alloy

It can be seen in Fig.7a that the microstructures comprises of B2-phase matrix, O-phase lamellae and a small amount of kinked and globularized O-phase when deforming at 930 and 950 °C. The O-phase lamellae are hard to be globularized due to the restricted atom diffusion and phase boundary migration at lower temperatures. In contrast, when the temperature increases to 970 °C, the amount of globularized O-phase particles has sharply increased. Therefore, the O-phase lamellae favor to globularize at higher temperatures owing to the larger recrystallization force. In addition, the diameter of globularized O-phase particles increases with the deformation temperature increasing, indicating its coarsening behavior during heating process, which is also beneficial to its further globularization.

Fig.7e~7f show the microstructures of the samples compressed at different strain rates at 950 °C and a height reduction of 70%. Generally, compared to the microstructure of the alloy compressed at a higher strain rate (1 s⁻¹ in Fig.7d), the O-phase lamellae are easier to be globularized at low strain rates (0.01 s⁻¹ in Fig.7f). This phenomenon accords well with that observed in Ti-5Al-5Mo-5V-1Cr-1Fe^[24] and Ti-6Al-4V^[25, 26] alloys.

It is well known that, the globularization may be rationalized to two aspects^[8, 25, 26]: break-up of lamellae and formation of globules. First, the nativity of interphase boundary which occurs at kinked (in Fig.8a) or sheared band (in Fig.8c) of lamellae is indispensable for the break-up of lamellae. This process is controlled by the effect of dislocation glide with the strain. The O-phase lamellae break up into discrete subgrains through intense shearing, as observed in Fig.8a and 8b. with larger imposed strains, more O-phase lamellae are sheared and globularized. The interface migration occurs by diffusional processes and the globular particles are formed. Thus it can be deduced that the globularization of the O-phase lamellae is a dynamic recrystallization behavior. The globularization behavior is hard to occur at low temperatures or high strain rates due to the slow diffusion rate or insufficient diffusion time. This

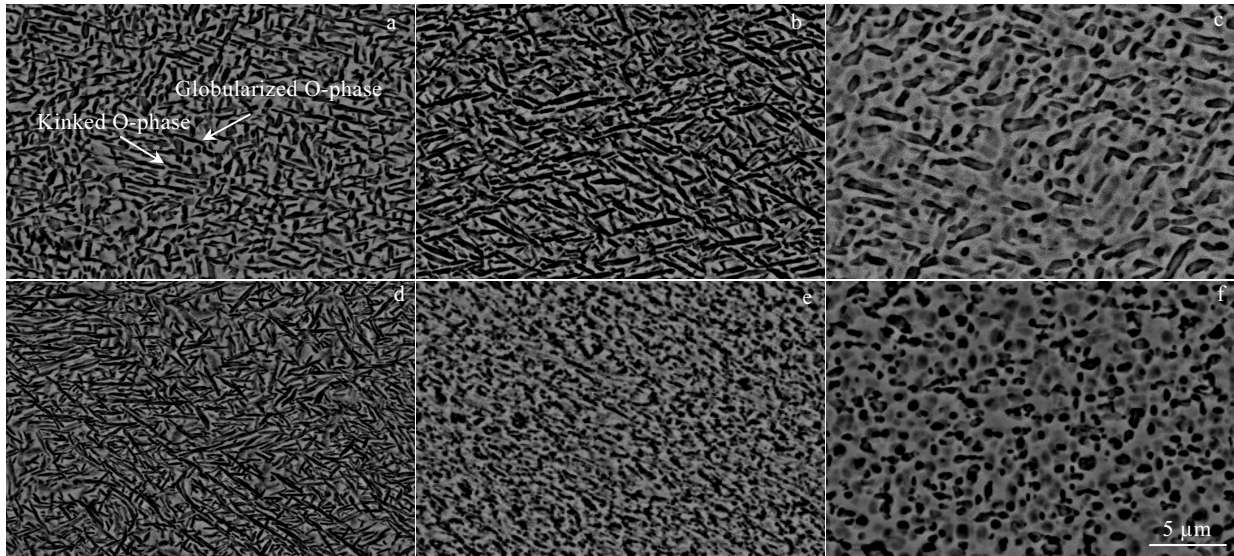


Fig.7 Microstructures of samples compressed at different temperatures with strain rate of 0.001 s^{-1} : (a) $930 \text{ }^{\circ}\text{C}$, (b) $950 \text{ }^{\circ}\text{C}$, (c) $970 \text{ }^{\circ}\text{C}$; at different strain rates at $950 \text{ }^{\circ}\text{C}$: (d) 1 s^{-1} , (e) 0.1 s^{-1} , and (f) 0.01 s^{-1}

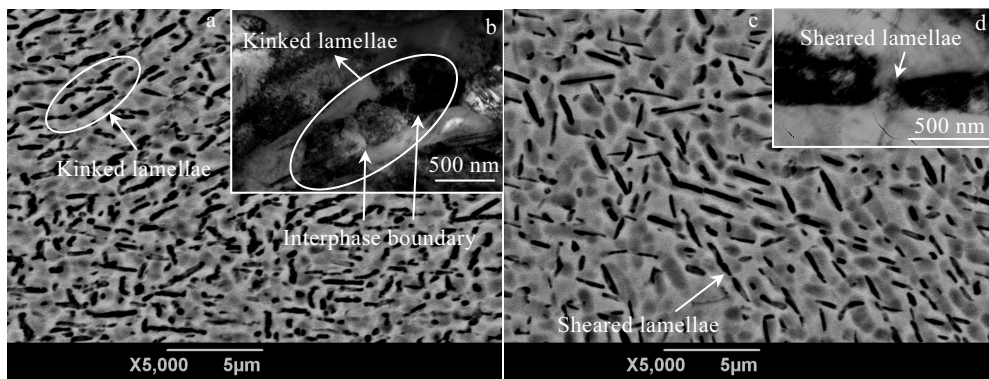


Fig.8 Globularization behavior of the O-phase lamella: (a, b) kinked lamellae and (c, d) sheared lamellae

diffusional process is driven by the urge to minimize the interfacial energy or the surface tension.

The fraction of dynamic globularized O-phase particles with strain at various strain rates and deformation temperatures are summarized in Fig.9. The results show that the globularization fraction is very sensitive to the deformation conditions and exhibits the sigmoid curves. Similar characteristics had been observed for Ti-6.5Al-3.5Mo-1.5Zr-0.3Si alloy^[27]. The dependence of the fraction of dynamic globularized O-phase particles on strain can be described by the equation

$$f_{Dg} = 1 - \exp[-k(\varepsilon - \varepsilon_c)^n] \quad (4)$$

where f_{Dg} is the volume fraction of dynamic globularized O-phase particles, ε_c is the critical strain for initiation of dynamic globularization, n is the Avrami-exponent, and k is the kinetic constant and temperature-dependent factor.

Non-linear curves fitting using Eq. (4) shows great agreements with the experimental results observed in Fig.9. Thus, the kinetics of dynamic globularization for the current alloy can be well described by Avrami type Eq.(4). The increase of the deformation temperature increases the values of parameters k and n . In addition, the values of parameters n decrease with the strain rate increasing. Moreover, the values of ε_c for the initiation of globularization are in the range of $0.02 \sim 0.17$ and decrease with the increase of temperature and decrease of strain rate. It accords well with the microstructure investigation in Figs.7~8. This phenomenon was also found in Refs.^[26-28], which reported that the critical strains for initiation of globularization are about $0.75 \sim 1.0$ for Ti-6Al-4V alloys and are all higher than the predicted values in this study. The Ti_2AlNb -based alloy seems easier to be globularized due to the thinner lamella for the initial microstructure.

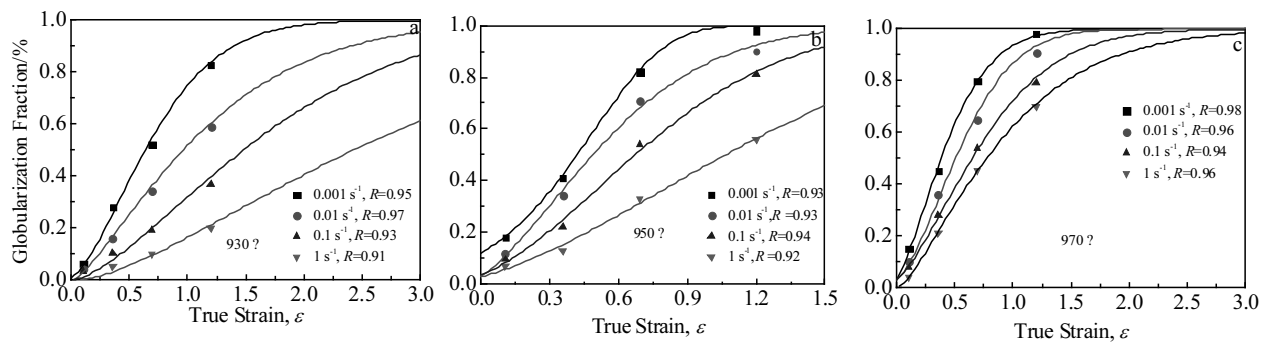


Fig.9 Fraction of globularized O-phase as a function of strain at various strain rates and deformation temperatures (dot: experimental data, line: fitting results using Eq. (4), R is the relevance between the experimental and fitting results)

3 Conclusions

1) The discontinuous yielding and flow softening of Ti-22Al-25Nb alloy can be observed from the stress-strain curves. The flow softening is relevant to dynamic globularization of O-phase lamellae and flow instability including 45° shear deformation, 45° shear cracking and free-surface cracking.

2) A deformation constitutive model based on the exponential law is developed to describe the deformation temperature and strain rate dependence of the flow stress. The deformation activation energy in (α_2 +O+B2) region is calculated to be $831 \text{ kJ}\cdot\text{mol}^{-1}$.

3) The globularization consists of two aspects including break-up of lamellae and formation of globules. The O-phase lamellae break up into discrete equiaxed O-phase particles through intense shearing. The globularization of the O-phase lamellae is confirmed to be a dynamic recrystallization behavior.

4) High temperature or low strain rate is beneficial to the globularization of the O-phase lamellae owing to the larger recrystallization force and sufficient recrystallization time. The size of globularized O-phase particles increases with the deformation temperature increasing.

5) The kinetics of dynamic globularization for Ti_2AlNb based alloy can be well described by the Avrami type. Compared to the traditional titanium alloy, the alloy is easier to be globularized due to the thinner lamella for the initial microstructure.

References

- Banerjee D, Gogia A K, Nandi T K et al. *Acta Metallurgica*[J], 1988, 36(4): 871
- Kumpfert J. *Advanced Engineering Materials*[J], 2001(3): 851
- Germann L, Banerjee D, Guédou J Y et al. *Intermetallics*[J], 2005, 13(9): 920
- Dang W, Li J S, Zhang T B et al. *Rare Metal Materials & Engineering*[J], 2015, 44(2): 261
- Lin P, He Z B, Yuan S J et al. *Materials Science & Engineering A* [J], 2012, 556(11): 617
- Yang K L, Huang J C, Wang Y N. *Acta Materialia*[J], 2003, 51(9): 2577
- Boehlert C J, Majumdar B S, Seetharaman V et al. *Metallurgical & Materials Transactions A*[J], 1999, 30(9): 2305
- Lin P, He Z B, Yuan S J et al. *Journal of Alloys & Compounds*[J], 2013, 578(1): 96
- Semiatin S L, Kirby B C, Salishchev G A. *Metallurgical & Materials Transactions A*[J], 2004, 35(9): 2809
- Muraleedharan K, Gogia A K, Nandy T K et al. *Metallurgical Transactions*[J], 1992, 23(2): 401
- Grylls R J, Banerjee S, Perungulam S et al. *Intermetallics*[J], 1998, 6(7-8): 749
- Weiss I, Semiatin S L. *Materials Science & Engineering A*[J], 1998, 243: 46
- Jonas J J, Heritier B, Luton M J. *Metallurgical Transactions A*[J], 1979, 10(5): 611
- Ankem S, Shyue J G, Vijayshankar M N et al. *Materials Science & Engineering A*[J], 1989, 111: 51
- Robertson D G, Mcshane H B. *Materials Science & Technology*[J], 1997(7): 575
- Li A B, Huang L J, Meng Q Y et al. *Materials & Design*[J], 2009, 30(5): 1625
- Jia W J, Zeng W D, Liu J R et al. *Materials Science & Engineering A*[J], 2011, 530(12): 135
- Zhu Y C, Zeng W D, Feng F et al. *Materials Science & Engineering A*[J], 2011, 528: 1757
- Pilehva F, Zarei-Hanzaki A, Ghambari M et al. *Materials & Design*[J], 2013, 51(5): 457
- Nandy T K, Banerjee D. *Intermetallics*[J], 2000(8): 1269.
- Tang F, Nakazawa S, Hagiwara M. *Scripta Materialia*[J], 2000, 43(12): 1065
- Nandy T K, Banerjee D. *Intermetallics*[J], 2000(8): 915
- Seshacharyulu T, Medeiros S C, Frazier W G et al. *Materials Science & Engineering A*[J], 2000, 284: 184
- Zherebtsov S V, Murzinova M A, Klimova M V et al.

- Materials Science & Engineering A*[J], 2013, 563: 168
- 25 Zherebtsov S, Murzinova M, Salishchev G et al. *Acta Materialia* [J], 2011, 59(10): 4138
- 26 Semiatin S L, Seetharaman V, Weiss I. *Materials Science & Engineering A*[J], 1999, 263(2): 257
- 27 Song H W, Zhang S H, Cheng M. *Journal of Alloys & Compounds*[J], 2009, 480: 922

Ti-22Al-25Nb (at%)合金 O 相层片高温变形动态球化行为

林 鹏^{1,2}, 唐婷婷¹, 池成忠^{1,2}, 张树志^{1,2}, 张长江^{1,2}

(1. 太原理工大学 材料科学与工程学院, 山西 太原 030024)

(2. 太原理工大学 先进镁基材料山西省重点实验室, 山西 太原 030024)

摘 要: 为阐明 Ti₂AlNb 基合金高温变形过程中 O 相层片的球化机制及模型, 研究了 Ti-22Al-25Nb (at%)合金在(α_2 +O+B2)相区压缩变形行为及显微组织演变规律。结果表明, 合金的软化行为与 O 相层片动态球化、45°方向剪切变形失稳及裂纹萌生有关。O 相层片在较低温度和较高应变速率下难以球化是由于原子具有较低的扩散速率和较短的扩散时间。O 相层片的球化机制主要为层片扭结和剪断, 本质上属于动态再结晶行为。建立了合金高温变形本构关系, 并计算了变形激活能为 831 kJ·mol⁻¹; 对 O 相层片球化的动力学过程进行了研究, 其动力学行为受变形条件影响很大, 遵循阿夫拉米曲线方程。

关键词: Ti₂AlNb 合金; 动态球化; 动态再结晶; 热变形

作者简介: 林 鹏, 男, 1982 年生, 博士, 讲师, 太原理工大学材料科学与工程学院, 山西 太原 030024, E-mail: linpeng@tyut.edu.cn